Ag nanoparticle-based efficiency enhancement in an inverted organic solar cell

Dalila Salem [1,2], Manal Shalabi [2], Fathi Souissi [3], Farida Nemmar [1], Mohammed Said Belkaid [1], Muhammad Aamir [4], and Jean-Michel Nunzi [2,3]

1. *Laboratory of Advanced Technologies of Genie Electrics (LATAGE), Faculty of Electrical and Computer Engineering, Mouloud Mammeri University (UMMTO), BP 17 RP 15000, Tizi-Ouzou, Algeria.*
2. *Department of Chemistry, Queens University, Kingston, Ontario, Canada.*
3. *Department of Physics, Engineering Physics and Astronomy, Queens University, Kingston, Ontario, Canada.*
4. *Materials Laboratory, Department of Chemistry, Mirpur University of Science and Technology (MUST), Mirpur-10250 (AJK), Pakistan*

Abstract

Herein, we demonstrate the improvement in performance of inverted organic solar cells fabricated with an Ag-nanoparticle (NP) modified ZnO-electron transport layer. Ag NP incorporation into the ZnO layer increases light harvesting efficiency of the solar device which untimely improves J_{SC} of the device. As a result, power conversion efficiency (PCE) of ZnO + Ag Np buffer layer based (ITO/ZnO:Ag NP/P3HT: PCBM/MoO3/Ag) device reaches 3.02 % which is 27 % higher than ITO/ZnO/P3HT: PCBM/ MoO3/Ag device and 55.6 % higher than the electron transfer layer(ETL) free (ITO/P3HT: PCBM/ MoO_3/Ag) control device.

Keywords: organic solar cell, inverted structure, electron transport layer, silver nanoparticles, Ag-NP doped ZnO.

1. INTRODUCTION

Easy solution process, eco-friendly, cost effective and potential for roll-to-roll fabrication make organic solar cells (OSCs) and attractive technology.[1-3] However, OSCs have limited light absorption due to small excitons diffusion length of about 10 nm and low carrier mobility. [4-6] To overcome these issues, several approaches were adopted to enhance the light absorption such as solvent addition,[7,8] use of suitable donor/acceptor polymer,[9] compositional tuning,[10] thermal annealing[8] and architectural modifications.[11]

Beside these approaches, the incorporation of metal oxides or suitable semiconductors into the light harvesting active layer was also adopted to enhance light trapping.[12-15] Apart from this strategy of enhancing the absorption/scattering of active layer, another strategy to enhance the efficiency of the OSCs is to modify the electrons or hole transporting layers.[16] Modification in the electron transport layer (ETL) increases charge carrier transport towards the electrodes and reduces charge carrier recombination that further enhances the performance of OSCs.[17]

In inverted OSCs, n-type metal oxides such as ZnO electron transport layer (ETL) are used. ZnO can be an excellent buffer layer with acceptable conductivity and transparency in the visible range and with enhanced chemical/thermal stability in different environments.[18,19] Metal nanoparticles (NP)

with surface plasmonic resonance (LSPR) have appeared to be a promising material for enhancement in OSCs optical performances. LSPR based light harvesting ability is often attributed to increased light pathway.[20,21]

In this work, we explore the effect of Ag Np on the light absorption and photovoltaic performance of inverted OSCs based on the poly (3-hexylthiophene): phenyl C_{61}-butyric acid methyl ester (P3HT: PCBM) active layer with ZnO buffer layer. The Ag Np modified ZnO buffer layers could improve device performance. The 40 nm sized Ag Np were synthesized using chemical reduction and characterized by absorption spectroscopy and transmission electron microscopy. The blend of ZnO and Ag Np was used as buffer layer to explore the OSCs performance. By incorporation of Ag Np in ZnO buffer layer, we have improved the performance of OSCs as the highest J_{sc} of 9.88 mA/cm^2, 560 mV and PCE of 3.02 %. Absorption enhancement in device with the dispersal of Ag Np in ZnO buffer layer (ETL) is attributed to LSPR effect, which increases the short-circuit current density (Jcs).

2. EXPERIMENTAL SECTION

Materials

Silver nitrate, trisodium citrate, sodium borohydride, Cetyl Trimethyl Ammonium Bromide (CTAB), ascorbic acid, sodium hydroxide P3HT and $PC_{61}BM$, 1,2-dichlorobenzene (1,2-DCB), and molybdenum oxide were purchased form sigma Aldrich and used without further purification.

Characterization

A Hitachi H-7000 transmission electron microscope (TEM) operating at a 75 kV accelerating voltage was used to evaluate the size and shape of the as-prepared Ag Np. Ultraviolet-visible (UV-vis) absorbance were measured using Hewlett Packard 8452A Diode Array Spectrophotometer at room temperature. The atomic force microscopy (AFM) images of various film surfaces were measured by a Veeco MultiMode scanning probe microscope operating in the tapping mode. The X-ray diffraction spectra of ZnO with and without Ag-Np films were obtained by X-ray diffraction with a Cu Ka X-ray tube (λ = 1.5406 Å). The current density-voltage (J-V) characteristics under dark and illumination (100 mW/cm^2) were recorded with a Keithley 2400 source measurement unit. The light intensity of the solar simulator was calibrated with a standard photovoltaic (PV) reference cell. External Quantum Efficiency (EQE) was recorded with a QEX 7 PV Measurement system in air.

Ag Nanoparticle Synthesis

Ag Np were synthesized with previously reported method.[22] Briefly, 250 µM of $AgNO_3$ and 250 µM of trisodium citrate were dissolved in 10 mL of D.I water under stirring. The 0.6 mL of (10 mM) $NaBH_4$ solution was injected swiftly into the mixture solution under vigorous stirring. The resultant solution was then used as seeds for growth of Ag Np. For growth of Ag Np, 0.4 mL of seed solution was injected into the solution of 0.29 g of CTAB, 250 µM $AgNO_3$ (10 mL) and (0.5 mL) 0.1 M ascorbic acid. In the final step, 0.1 mL of 4 mM NaOH was added to get the Ag Np.

Device fabrication

Inverted OSCs were fabricated on pre-patterned ITO glass substrates (around 2 × 2.5 cm2 in size, 15

Ω per square, with 135 ± 15 nm ITO film thicknesses). The patterned ITO glass substrates were sequentially cleaned with detergent powder, distilled water, acetone and isopropyl alcohol for 10 min each. The substrates were heated at about 100 °C for 5 min, dried substrates were further cleaned 15 min in a plasma cleaner. As-prepared Ag Np aqueous solutions with an intermediate concentration were blended into the ZnO solution at 2 % V/V. After that, on the top of the ITO substrates, the ZnO and ZnO + Ag Np solution was then spin-coated at 3500 rpm for 40 s, annealing at 200°C for 30 min in air. Subsequently, the substrates were transferred into a nitrogen-filled glove box. The active layer solution of P3HT and PC61BM blend with a weight ratio of 1:08 in 1,2-dichlorobenzene (1,2-DCB) (20 mg/mL of P3HT and 16 mg/mL PCBM). The blend solution was spin-coated on the ZnO layer at 600 rpm for 50 s, and the active layer was annealed at 110 °C for 10 min. Finally, the devices were finished by thermal evaporation of 5 nm MoO_3 layer and 100 nm Ag electrode. The device area is 6 mm^2.

3. RESULTS AND DISCUSSION

Figure 1a shows the TEM image of as-prepared Ag Np: they have a spherical shape with uniform size distribution. The histogram of size distribution in figure 1b yields 40 ± 5 nm Ag Np. UV-vis absorption spectrum of Ag Np in figure 1c further confirm the Ag Np formation. The as-prepared Ag Np show the absorption maxima at around 442 nm which is attributed to the LSPR effect of Np.[23,24]

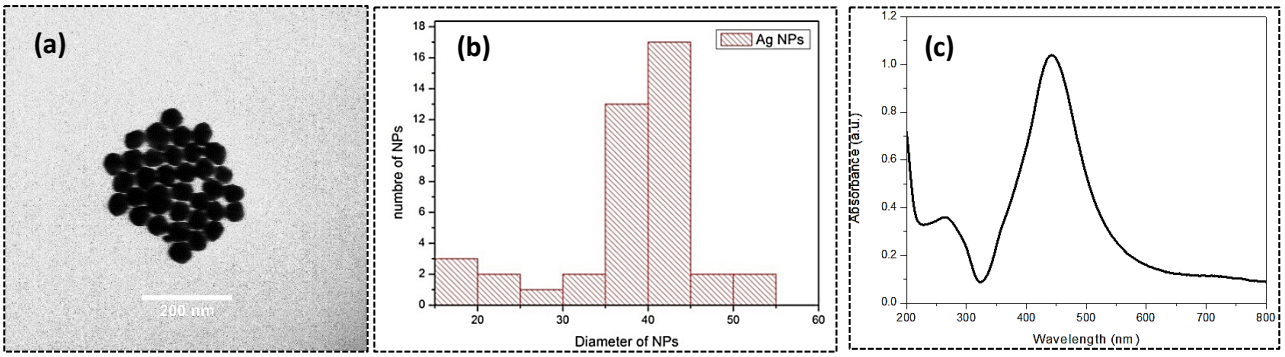

Figure 1. (a) TEM Image, (b) histogram for size distribution based on TEM image and (c) UV-vis absorption spectrum of as-prepared Ag Np dispersed in aqueous solution.

As-prepared Ag Np were then mixed with ZnO and deposited as thin films for solar cell application. Powder XRD analysis was performed for ZnO thin films and ZnO, Ag Np blended thin films as shown Figure 2. The pure ZnO thin film has diffraction peaks matching with the hexagonal wurtzite phase of ZnO. The incorporation of Ag Np in ZnO does not show any change in the crystalline phase of ZnO owing to the small NP-load.

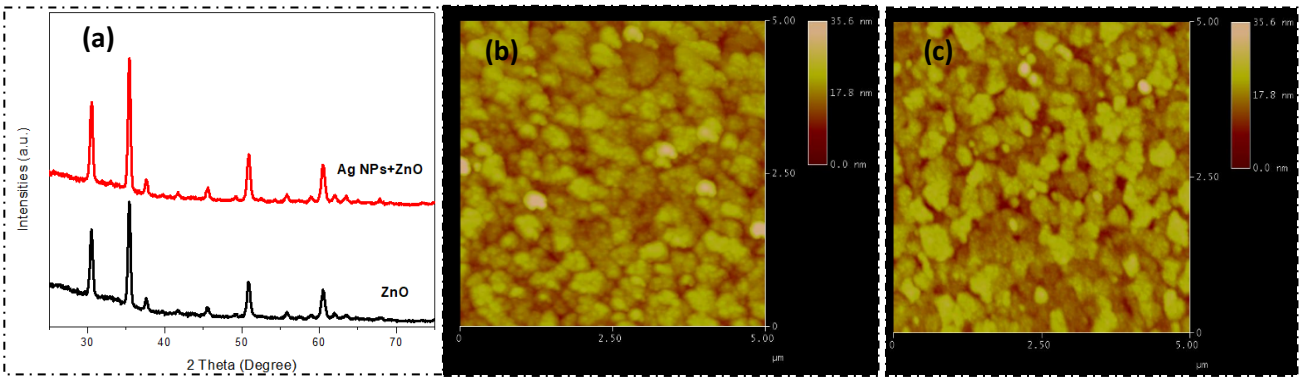

Figure 2. (a) Comparative pXRD patterns of pure ZnO and ZnO + Ag NP, (b) AFM image of pure ZnO film and (c) is the AFM image of ZnO + Ag NP films.

The surface morphology of pure ZnO and ZnO-Ag Np based thin films for ETL application was investigated by atomic force microscopy (AFM), as shown in Figure 2(c-d). The pure ZnO thin film was smoother than the ZnO + Ag NP film. The root-mean-square (RMS) value of ZnO (Figure 2b) was found to increase from 3.18 nm for pure ZnO to 3.45 nm for ZnO +Ag NP thin film (Figure 2c). The roughness of ETL is important to develop an efficient interface between ETL and active layer that helps increase the electron collection efficiency with high J_{SC}.[25]

Device architecture is shown in figure 3a. The photovoltaic parameters of all devices with ITO/P3HT: PCBM/ MoO_3/Ag (Control), ITO/ZnO/P3HT: PCBM/ MoO_3/Ag (ZnO based) and ITO/ZnO: Ag Np/P3HT: PCBM/MoO_3/Ag (ZnO + Ag NP) are extracted from current voltage characteristics in figure 3b. Results are summarized in Table 1. The OSCs with ZnO + Ag NP based ETL show a significant improvement of around 27 % compared to pure ZnO based device and 55.6% from the ETL free control device. The incorporation of Ag NP into the ZnO based ETL, the device has shown an average J_{sc} of 9.88 mA/cm^2, V_{oc} of 560 mV and FF of 55.69% results in a high-power conversion efficiency (PCE) of 3.02 %.

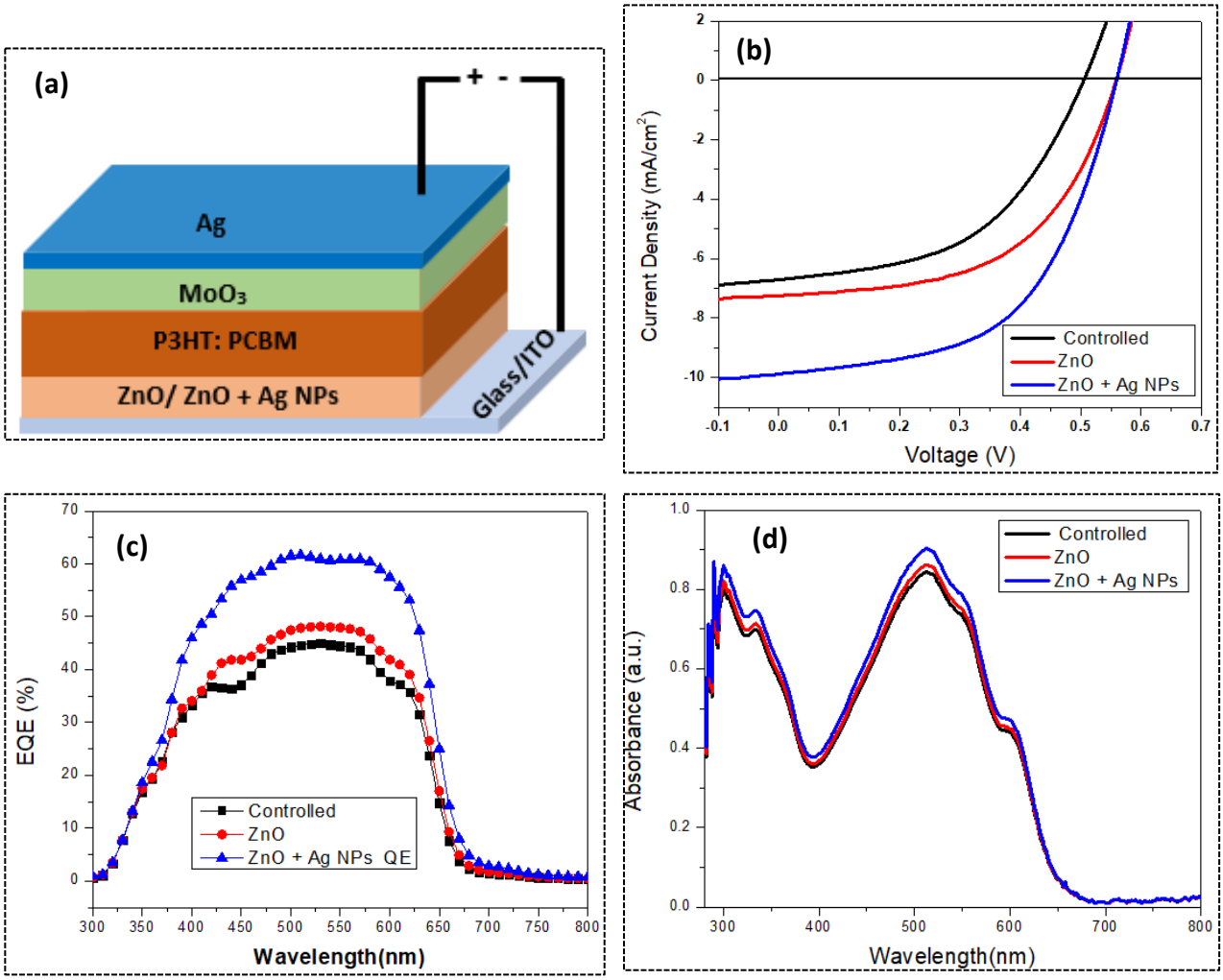

Figure 3. (a) Inverted organic solar cells device architecture (b) comparative J-V curve of the P3HT:PC_{61}BM devices with ETL free (Control), with ZnO ETL layer and with ZnO + Ag NP ETL.

Monotonic increase in photovoltaic performance from control device to ZnO ETL-based to Ag Np incorporated ZnO based devices is observed. Low performance in control ITO/P3HT: PCBM/ MoO_3/Ag) device is due to poor ohmic contact of the active layer with the electrode. The improvement of performances upon adding a ZnO as ETL layer (ITO/ZnO/P3HT:PCBM/ MoO_3/Ag) results in J_{sc} increase to 7.24 mA/cm^2 and a fill factor (FF) of 53.99 %. Increased FF is attributed to reduced charge recombination with the improvement in interface contact between ETL and active

layer. The Ag Np incorporated ZnO ETL based ITO/ZnO: Ag Np/P3HT: PCBM/MoO_3/Ag device shows lowest series resistance (Rs). Thus, enhanced PCE with improved J_{sc} in OSCs is attributed to the plasmon resonance on Ag Np that boots the performance of photovoltaic devices

Table 1. photovoltaic parameters of average values of all as-fabricated devices.

Device	**V_{co} (v)**	**J_{sc} (mA cm^{-2})**	**FF (%)**	**Rs (Ω cm^2)**	**R_{sh} (Ω cm^2)**	**PCE %**
Control	0.50	-6.71	0.50	23.45	532.50	1.68 ± 0. 2
ZnO	0.56	-7.24	53.99	16.03	595.74	2.19 ± 0. 1
ZnO + Ag Np	0.56	-9.88	54.69	12.18	559.32	3.02 ± 0.1

The external quantum efficiency (EQE) spectrum of as-fabricated solar devices (Control, ZnO based and ZnO + Ag Np ETL based) is shown in Figure 3c. A maximum EQE of 44.29% is observed for the ZnO ETL free device (Control), whereas, the device with ZnO ETL layer has maximum EQE of 47.44 % in the wavelength range of 400-550 nm. Significant enhancement in EQE is observed in the device with ZnO incorporated with Ag Np based ETL layer with highest value of 61.64% in the wavelength range of 400-550 nm. EQE enhancement by the Ag Np incorporated ZnO ETL based device is explained by light harvesting.[26]

The absorption spectra of active layers with/without ZnO ETL layer and ZnO + Ag Np ETL layers Is given in figure 3d. Absorbance is higher for the active layer with ZnO + Ag Np ETL in the wavelength range 400-600 nm compared to the device with and without ZnO ETL layer. The P3HT:PCBM layers with and without ZnO closely resemble each other, however slightly higher absorption can be observed around 380 nm in the film with ZnO layer. This absorption is due to the ZnO layer that absorb in this region with direct bandgap of ~3.34eV.[26] whereas, the absorption enhancement for device with Ag-Np into the ZnO ETL layer is attributed to LSPR scattering by the Ag Np.[27]

4. CONCLUSION

Ag Np modified ZnO buffer layers were fabricated by blending with as-prepared Ag Np. The Ag Np were prepared by chemical reduction of $AgNO_3$ in aqueous solution. The OSCs based on ZnO modified with Ag Np show the PCE of 3.02 % which is 27 % higher than the OSC based on pure ZnO buffer layer and 55 % higher compared to buffer layer free device. Incorporation of Ag Np into the ZnO buffer clearly enhances light absorption in the visible range.

AUTHOR CONTRIBUTION STATEMENT

FN, MSB and JMN supervised the project. DS, MS and FS conducted the experiments: NP synthesis and analysis (MS), sample fabrication (FS) and PV measurements (DS). DS, MS, FS and JMN carried the data analysis. DS drafted the manuscript with input from MS and MA. All authors reviewed and approved the submission.

AKNOWLEDGEMENT

This research was supported by Mouloud Mammeri Tizi Ouzou (Ageria) and the Chemistry

Department at Queen's University. We acknowledge support from the National Science Research Council of Canada Discovery Grants (RGPIN-2015-05485).

REFERENCES

1. G. Yu, J. Gao, J. C. Hummelen, F. Wudl and A. J. Heeger, *Science*, 1995, **270**, 1789-1791.
2. U. Jabeen, T. Adhikari, S. M. Shah, D. Pathak, V. Kumar, J.-M. Nunzi, M. Aamir and A. Mushtaq, *Chinese Journal of Physics*, 2019, **58**, 348-362.
3. F. C. Krebs, *Solar energy materials and solar cells*, 2009, **93**, 394-412.
4. S. R. Gollu, R. Sharma, G. Srinivas, S. Kundu and D. Gupta, *Organic Electronics*, 2016, **29**, 79-87.
5. P. W. M. Blom, V. D. Mihailetchi, L. J. A. Koster and D. E. Markov, *Advanced Materials*, 2007, **19**, 1551-1566.
6. V. Shrotriya, E. H.-E. Wu, G. Li, Y. Yao and Y. Yang, *Applied physics letters*, 2006, **88**, 064104.
7. C. V. Hoven, X. D. Dang, R. C. Coffin, J. Peet, T. Q. Nguyen and G. C. Bazan, *Advanced Materials*, 2010, **22**, E63-E66.
8. W. Ma, C. Yang, X. Gong, K. Lee and A. J. Heeger, *Advanced Functional Materials*, 2005, **15**, 1617-1622.
9. Y.-C. Huang, Y.-C. Liao, S.-S. Li, M.-C. Wu, C.-W. Chen and W.-F. Su, *Solar Energy Materials and Solar Cells*, 2009, **93**, 888-892.
10. D. H. Wang, J. K. Kim, O. O. Park and J. H. Park, *Energy & Environmental Science*, 2011, **4**, 1434-1439.
11. S. Sista, M. H. Park, Z. Hong, Y. Wu, J. Hou, W. L. Kwan, G. Li and Y. Yang, *Advanced materials*, 2010, **22**, 380-383.
12. H.-C. Liao, C.-S. Tsao, T.-H. Lin, M.-H. Jao, C.-M. Chuang, S.-Y. Chang, Y.-C. Huang, Y.-T. Shao, C.-Y. Chen, C.-J. Su, U. S. Jeng, Y.-F. Chen and W.-F. Su, *ACS Nano*, 2012, **6**, 1657-1666.
13. M. A. García, *Journal of Physics D: Applied Physics*, 2011, **44**, 283001.
14. S.-W. Baek, J. Noh, C.-H. Lee, B. Kim, M.-K. Seo and J.-Y. Lee, *Scientific reports*, 2013, **3**, 1726.
15. J. R. Cole and N. Halas, *Applied physics letters*, 2006, **89**, 153120.
16. S. K. Hau, H.-L. Yip, N. S. Baek, J. Zou, K. O'Malley and A. K.-Y. Jen, *Applied Physics Letters*, 2008, **92**, 225.
17. M. A. Ibrahem, H.-Y. Wei, M.-H. Tsai, K.-C. Ho, J.-J. Shyue and C. W. Chu, *Solar Energy Materials and Solar Cells*, 2013, **108**, 156-163.
18. M. Aamir, T. Adhikari, M. Sher, N. Revaprasadu, W. Khalid, J. Akhtar and J.-M. Nunzi, *New Journal of Chemistry*, 2018, **42**, 14104-14110.
19. S. K. Hau, H.-L. Yip, O. Acton, N. S. Baek, H. Ma and A. K.-Y. Jen, *Journal of Materials Chemistry*, 2008, **18**, 5113-5119.
20. V. Rivera, F. Ferri and E. Marega Jr, *Plasmonics-Principles and Applications*, 2012, 283-312.
21. X. Fan, W. Zheng and D. J. Singh, *Light: Science & Applications*, 2014, **3**, e179-e179.
22. N. R. Jana, L. Gearheart and C. J. Murphy, *Chemical Communications*, 2001, 617-618.
23. L. Lu, Z. Luo, T. Xu and L. Yu, *Nano Letters*, 2013, **13**, 59-64.
24. H. Zhao, F. Huang, J. Hou, Z. Liu, Q. Wu, H. Cao, Q. Jing, S. Peng and G. Cao, *ACS applied materials & interfaces*, 2016, **8**, 26675-26682.
25. K. N'Konou, M. Chalh, V. Monnier, N. P. Blanchard, Y. Chevolot, B. Lucas, S. Vedraine and P. Torchio, *Synthetic Metals*, 2018, **239**, 22-28.
26. A. Schleife, F. Fuchs, J. Furthmüller and F. Bechstedt, *Physical Review B*, 2006, **73**, 245212.
27. L. Feng, M. Niu, Z. Wen and X. Hao, *Polymers*, 2018, **10**, 123.